Acta Geochim (2022) 41(4):717–729
https://doi.org/10.1007/s11631-022-00539-w

ORIGINAL ARTICLE

Petrogenesis of the Lunar volcanic glasses and Mg-suite: constraints on a post-magma-ocean cumulate overturn

Rui Li[1,2,3,4] · Wei Du[2,4] · Jing Yang[1]

Received: 4 January 2022 / Revised: 24 March 2022 / Accepted: 27 March 2022 / Published online: 14 May 2022

Abstract The lunar volcanic glasses and Mg-suite rocks represent the early enigmatic episodes of lunar magmatism. Due to the gravitational instability of the Fe–Ti enriched (± KREEP) layer, which is formed at the later stage of fractional crystallization, a post-magma-ocean cumulate overturn occurred contemporaneously or near-contemporaneously with the lunar magma ocean (LMO) solidification. The radioactive elements within the KREEP layer were transferred downward and provided continuous energy for the partial melting of the Moon's interior. The melt from the Moon's interior and those from decompression melting, in turn, provide source magma for the origin of lunar volcanic glasses and Mg-suite. However, experimental and theoretical studies on the formation process of lunar volcanic glasses and Mg-suite show that the origin of their parental magma is poorly constrained, which largely depends on the initial depth and composition of the LMO. This review examines the mineralogy, petrogenesis, and distribution of lunar volcanic glasses and Mg-suite. Combining with existing models, we constrain the degree, distribution, and timescale of lunar mantle overturn and explore their relationship with later stages of LMO differentiation. We propose an updated chemical composition of the lunar interior, which provides a useful reference for estimating the bulk composition and early differentiation of the Moon and the early Earth.

Keywords Lunar magma ocean · Overturn · Lunar volcanic glasses · Mg-suite

✉ Wei Du
duwei@mail.gyig.ac.cn

[1] Center for Lunar and Planetary Sciences, Institute of Geochemistry, Chinese Academy of Sciences, 550081 Guiyang, China

[2] State Key Laboratory of Ore Deposit Geochemistry, Institute of Geochemistry, Chinese Academy of Sciences, 550081 Guiyang, China

[3] University of Chinese Academy of Sciences, 100049 Beijing, China

[4] Center for Excellence in Comparative Planetology, Chinese Academy of Sciences, 230026 Hefei, China

1 Introduction

The Moon experienced extensively melting due to the high energy from the Moon-forming giant impact. The concept of the Magma Ocean was introduced to the Moon to explain the genesis of the plagioclase, which accounts for about 75% of the lunar surface (Smith et al. 1970; Wood et al. 1970). Subsequently, a series of lunar magma ocean (LMO) models appeared to describe the crystallization sequence of the silicate Moon and explain the petrogenesis of collected lunar samples (Drake 1976; Ringwood 1975; Taylor 1975; Walker and Hays 1977; Wood 1972). These models generally agree that a variety of mafic lithologies (olivine and orthopyroxene) were produced at the early stage of the LMO crystallization and formed a heterogeneous mantle, followed by plagioclase, which floated to the top of the magma ocean and formed a ferroan anorthosite primary crust. Through the LMO crystallization, incompatible elements, including potassium (K), rare earth elements (REEs), phosphorus (P) etc. gradually enriched in the residual melt, and finally formed urKREEP between the crust and the mantle (Neal 2001; Walker and Hays 1977; Warren 1985). And the model age ~ 4.2 Ga of KREEP marks the completion of LMO crystallization (Nyquist and

Shih 1992). At the ending period of LMO crystallization, the last-formed, subcrustal cumulate assemblages are Fe- and Ti-rich and hence denser than the early formed cumulate, leading to gravitational instability. This instability will result in overturn of cumulate piles, bringing KREEP-bearing materials to depth and raising less dense refractory materials to shallower levers, promoting remelting of the mafic cumulates. The lunar mantle overturn, which caused longitudinal variations in composition and structure, is an important stage in the evolution of the Moon. Convective mixing and/or upwelling of mantle materials by this post-magma-ocean overturn can be probable sources of mare basalts (Brown and Grove 2015), which lasted about 2 Ga (Hiesinger and Head 2006; Shearer 2006). In the context of the LMO paradigm, lunar scientists have been successfully constrained the formation process of most of the lunar samples either by direct crystallization of LMO, such as ferroan anorthosites, or by partial melting of differentiated mantle materials, such as mare basalts, or by a mixture of internal components, such as volcanic glasses and Mg-suite. Therefore, studying volcanic glasses and Mg-suite can concretely constrain the distribution of ilmenite-bearing cumulates (± KREEP), the limitation of the depth of overturning, and the timescale of lunar mantle overturn.

Lunar ultramafic volcanic glasses were proposed to be formed by remelting a source region that consists of a mixture of mafic cumulates with ilmenite-bearing cumulates (± KREEP) of late-stage LMO through mantle overturn (Longhi 1992, 2006). If the ilmenite layer sank through the mantle during overturning introducing Fe–Ti-rich lithologies to the source of lunar volcanic glasses, the compositional variety of lunar volcanic glasses should provide information about the efficiency of lunar mantle overturn and the locations of Fe–Ti-rich zones inside the lunar mantle. In other words, the compositional variability makes lunar ultramafic glasses unique probes into the compositional structure of the lunar interior. Therefore, experimental studies on the petrogenesis of volcanic glasses offer constraints on the thermochemical evolution of the lunar interior, such as their parental material's constitution, degree of partial melting, and oxygen fugacity. However, the origin of parental magmas of lunar volcanic glasses is still uncertain. The inference of the origin of volcanic glasses is affected by the lithology of surrounding rock, which varies with the depth and composition of the LMO. In addition, the sinking depth and degree of melting of ilmenite-rich cumulates are also key issues. For example, moonquake data indicate that a partially molten layer exists at the Moon's core-mantle boundary (Nakamura 2005; Weber et al. 2011), and the source for the partial melt layer could be the overturned Fe–Ti-rich layer (Mallik et al. 2019; Yao and Liang 2012). However, due to incompressible at much higher pressures, the density of the Ti-rich liquids are smaller than the overlying mantle, indicating that these melts cannot sink nor stabilize at the core-mantle boundary (Vander Kaaden et al. 2015).

On the other hand, as important intrusive plutonic rocks, Mg-suite, are suggested to be produced by post-LMO secondary magmatism because of its high Mg# (> 78) and An# (plagioclase > An_{90}), but not crystallization product of the primary lunar magma ocean (Shearer et al. 2015). The Mg-suite's primary melt was proposed to be derived from a primitive mantle reservoir, such as olivine-dominated cumulates formed during the early stage of LMO crystallization (Elardo et al. 2011; Elkins-Tanton et al. 2011; Lin et al. 2017; Prissel and Gross 2020; Rapp and Draper 2018). And lunar mantle overturn brings those deep olivine-dominated cumulates to invade the upper mantle toward the lunar surface. Therefore, this extensive period of Mg-suite magmatism must be associated with an earlier magmatic pulse, constraining the timescale of the LMO solidification and overturn event. And also, the age of the Mg-suite should be younger than that of lunar rocks derived from LMO such as the ferroan anorthosites (FANs). However, several studies have shown overlapping chronology relationships between Mg-suite samples (4345 ± 15 Ma) and anorthosite (4359 ± 9 Ma) (Borg et al. 2017; Edmunson et al. 2009; Gaffney and Borg 2014). In addition, the discovery of KREEP-poor lunar meteorite with Mg-suite-like composition suggests that primitive sources for Mg-suite could be partial melts from the primitive lunar reservoir without KREEP-bearing parental melt (Prissel et al. 2014). If lunar mantle overturn was the driving force for melting of lunar primitive mantle reservoir, which accounts for the parental magma of Mg-suite, study on the formation mechanism of Mg-suite thus can help to constrain the timing and extent of lunar mantle overturn.

This study revisits post-LMO magmatism caused by mantle overturn in light of updated studies on the petrology, geochemistry, and distribution of the different types of volcanic glasses (low-Ti, intermediate-Ti, and high-Ti) and Mg-suite. We examine the effect of LMO depth on its lower mantle composition and propose a new explanation for the chemical characters of lunar volcanic glasses and the formation mechanism of the Mg-suite. These results can further constrain the bulk composition of the Moon, the extent of initial lunar melting, and the scale of lunar mantle overturn.

2 Petrogenesis of the lunar volcanic glasses

Volcanic glasses are rapidly quenched glass beads during pyroclastic fire fountain eruptions and differ from glasses formed by the impact on the lunar surface. The latter tends

to be chemically heterogeneous due to a lack of time to spread temperature to melt evenly (Delano 1986). It is generally believed that external impacts caused volcanic eruptions on the Moon, and basalt magma is squeezed up along the fissures and spewed out of the lunar surface (Solomon and Head 1980), or the presence of volatiles, such as C, H_2S, HF, and HCl, provided the driving force for magma eruption (Head and Wilson 1979; Sato 1979). However, there are studies show that volatile exsolution from the picritic melt is not an effective process for driving lunar pyroclastic eruptions (Fogel and Rutherford 1995), and the existence of volatiles are not helpful for negative buoyancy of magmatic melt to rise or erupt to the lunar surface either (Vander Kaaden et al. 2015). Nevertheless, the composition of glasses beads reflects the composition and depth of their source regions, although not as directly as we would like. To some extent, they are the representative products of a post-magma-ocean cumulate overturn. Therefore, many works focus on the composition and extent of various glasses source regions as a means of inferring the extent of early lunar differentiation.

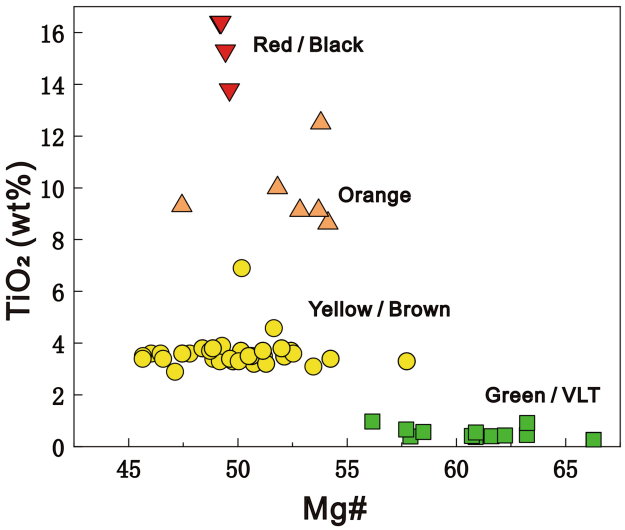

Fig. 1 Variation of TiO_2 content vs. Mg# [Mg# = molar Mg/(Mg + Fe) × 100] among some lunar volcanic glasses. Data are from Delano (1986) and Hughes et al. (1988)

2.1 Composition and significance

Volcanic glass beads are common in lunar samples, and normally show high FeO and MgO contents, but low Al_2O_3, CaO, and Na_2O contents (Table 1). Lunar volcanic glasses can be subdivided into three categories due to different titanium content corresponds to different colors (Fig. 1): (1) Low-titanium (low-Ti) and very-low titanium (VLT) glasses ($TiO_2 < 3$ wt%), includes Apollo 15 green glass (A15G, $TiO_2 \sim 0.2$–0.4 wt%); (2) Intermediate-titanium (Intermediate-Ti) glasses ($TiO_2 \sim 3$–7 wt%), such as Apollo 14 yellow glass (A14Y, TiO_2 = 4.58 wt%); (3) High-titanium (high-Ti) glasses ($TiO_2 > 7$ wt%), includes Apollo 17 orange glass (A17O, TiO_2 = 9.12 wt%), Apollo 15 red glass (A15R, TiO_2 = 13.8 wt%), and Apollo 14 black glass (A14B, TiO_2 = 16.4 wt%) (Brown and Grove 2015; Delano 1986; Papike et al. 1998). These glasses represent primary unfractionated melts, making them good candidates for studying the physical properties of lunar basalt and the partial melting process of the lunar mantle. Therefore, experiments on the multiple saturation phases of these glasses at different pressures can help to constrain the mineral composition and depth of their source regions. Together with sink–float experiments on synthetic compositional different lunar glasses, we can further determine the buoyancy and formation mechanism of these picritic melts, thus the structure of the lunar interior.

2.1.1 Low Ti glasses

The compositional trends of the Apollo 15 green glasses are distinctive and span a broad range, with Mg# from 60.6 to 67.4 (MgO from 17.1 to 18.6 wt%), SiO_2 from 45.5 to 48.5 wt%, TiO_2 from 0.42 to 0.23 wt%, and FeO from 20 to 16 wt%, and can be divided into groups A, B, and C, as defined by Delano (1979). The Apollo 15 C green glass has the highest Mg# among all the picritic glasses yet found on the Moon (Mg# = molar [Mg/(Mg + Fe)] × 100) (Delano

Table 1 Composition of the lunar volcanic glasses

	SiO_2	TiO_2	Al_2O_3	Cr_2O_3	FeO	MnO	MgO	CaO	Na_2O	K_2O	Mg#
Apollo15 Green C glass[a]	48.00	0.26	7.74	0.57	16.50	0.19	18.20	8.57	n.d.	n.d.	66.30
Apollo14 Yellow glass[a]	40.80	4.58	6.16	0.41	24.70	0.30	14.80	7.74	0.42	0.10	51.60
Apollo17 Orange glass[a]	38.50	9.12	5.79	0.69	22.90	n.a.	14.90	7.40	0.38	n.d.	53.70
Apollo15 Red glass[b]	35.60	13.80	7.15	0.77	21.90	0.25	12.10	7.89	0.49	0.12	49.60
Apollo14 Black glass[a]	34.00	16.40	4.60	0.92	24.50	0.31	13.30	6.90	0.23	0.16	49.20

n.a. not analyzed; *n.d.* not detected;

[a]Delano (1986); [b] Krawczynski and Grove (2012)

1979; Elkins-Tanton et al. 2003). These picritic glasses are considered to come from greater depths than mare basalts and play a dominant role in variable interpretations of lunar magmatism.

Considering the smallest Eu anomalies and the very low-Ti content, the 15 A glasses were interpreted to have no connection with KREEP, but most likely form from a less evolved lunar mantle cumulates. Phase equilibrium experiment combined with petrogenetic modeling results confirmed that the Apollo 15 A–B–C picritic glasses trend originated over a depth range of ~ 460 to ~ 260 km within the Moon but could not have been formed by fractional crystallization or any continuous assimilation/fractional crystallization (AFC) process. Instead, the 15 A glasses may have been formed by partial melting over a small pressure range at a particular depth (~ 440 km), the group B glasses are well modeled by starting with an intermediate A composition and assimilating a shallower cumulate, and the group C glasses were modeled by a second assimilation event (Elkins-Tanton et al. 2003). Meanwhile, sink-float experiments at different pressures confirmed that the molten A15C green glass was able to rise through the lunar mantle by buoyancy forces alone at 1.3 GPa (~ 260 km). If A15C originated from a greater depth, the melt would still buoyantly rise through the mantle as long as this depth did not exceed 2.8 GPa (~700 km) (Vander Kaaden et al. 2015). These studies on the original depth of the very low-Ti Apollo 15 green glasses are consistent with a relatively shallow LMO of about 500 km (Barr and Grove 2013), which may not be the case according to the latest moonquake data and geochemical exploration (Lognonne 2005; Nakamura et al. 1973; Warren 1985). In addition, Longhi (2006) carried out calculations to study the formation of picritic mare basalts with a variety of chemical compositions through different melting models (isobaric batch, polybaric batch, and polybaric fractional). His calculations support a deeper (700–1000 km) and low Al_2O_3 content source region without an aluminous phase for the green picritic glasses (Longhi 2006). However, our high-pressure (3.5 GPa and 1650 °C) crystallization experiments on glasses with LPUM composition show that the equilibrium crystallization product contains ~ 8 vol% pyrope-rich garnet and ~ 20% melt, indicating that the Al-rich phase (garnet) could be stable at the lower lunar mantle, thus the partial melting product of the lower lunar mantle with LPUM composition (~ 4 wt% of Al_2O_3) can be still low Al_2O_3 content (Fig. 2). The new experimental results indicate that Apollo 15 green glass may originate from deep inside the Moon and encourage us to reconsider the depth of LMO and the formation mechanism of lunar volcanic glasses.

The existence of garnet in the source region of lunar volcanic glasses has been suggested by other researchers.

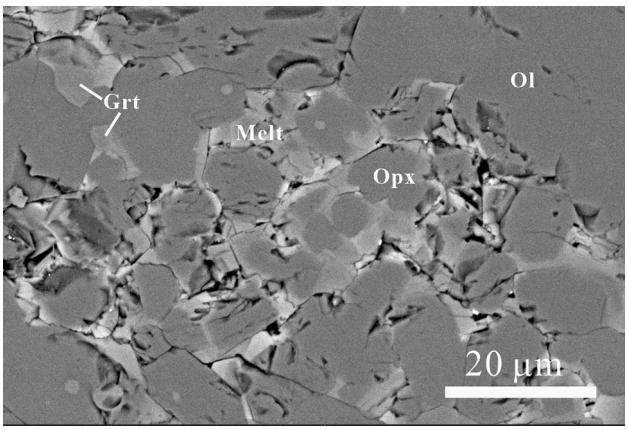

Fig. 2 SEM image of quenched products from equilibrium crystallization experiment on LPUM composition (3.5 GPa and 1650 °C) by piston-cylinder in this study. Ol—olivine; Opx—orthopyroxene; Grt—garnet

New inductively coupled plasma-mass spectrometry (ICP-MS) analysis on 65 high- and low-Ti Apollo mare basalts samples shows that some volcanic glasses exhibit the highest Sm/Yb ratio of ~ 2, which cannot be explained by mixing with KREEP (~ 1.5) (Fig. 3), implying that garnet was present in the source of these lunar glasses (Neal 2001). On the other hand, Khan et al. (2006) proposed that the most probable solution to the lunar seismic data yielded a lower lunar mantle consisting primarily of olivine (60%) and garnet (40%), although there was another feasible solution with less garnet and more pyroxene (Khan et al. 2006). Moreover, Elardo et al. (2011) showed that an LMO with refractory element enriched bulk composition could form a deep lunar mantle that contains garnet in addition to

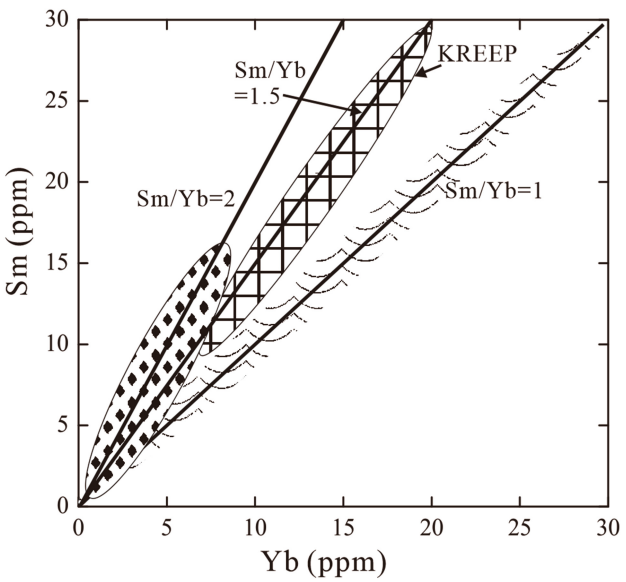

Fig. 3 Diagrams illustrating the role of garnet in the source regions of some volcanic glasses. Modified from Neal (2001)

low-Ca pyroxene and olivine (Elardo et al. 2011). In short, garnet is very likely to exist in the early Moon interior and have a non-negligible impact on the sources of lunar volcanic glasses.

Draper et al. (2006) did multiple saturation experiments on A15C and showed that it was saturated with garnet and pyroxene on the liquidus between 3.0 and 3.5 GPa. However, using the partitioning coefficient of rare earth elements between garnet and the coexisting melt, they suggested that garnet is unlikely to be present in the source for very Ti-poor lunar melts (A15C glass) (Draper et al. 2006). It is worth noting that the garnets obtained in their near-liquidus phase experiments are Fe-rich (FeO wt% =10.13–15.63) and show some majorite component, which is quite different compared with pyrope obtained by the crystallization experiments in Elardo et al. (2011). The partitioning coefficient of REEs between garnet and silicate liquid changes with the composition of garnet (Draper et al. 2003; Du et al. 2017). Therefore, extensive experiments are needed to verify the effect of garnet on the fractionations of REE during lunar mantle fractionation and lunar magmatic activities. Barr and Grove (2013) carried out phase equilibrium experiments to study the origin of the A15A glass and proposed that it was formed through a mixing process involving melt derived from the primitive garnet-bearing undifferentiated mantle (20%), and melt from late-stage magma ocean cumulates (80%) (Barr and Grove 2013). In their model, the lunar mantle overturn transferred Fe-rich cumulate to the bottom of the LMO and the undifferentiated primordial lunar interior did not participate in the lunar mantle overturn process but got heated to convective overturn by an imagined core dynamo. The adiabatic decompression melting of the undifferentiated lunar lower mantle assimilated the cumulate at the bottom of LMO to form the magma source of A15A glass. Along this line, the formation mechanism of lunar low-Ti glasses provides information on the depth and composition of the LMO and the scale of lunar mantle overturn.

In short, although very low-Ti Apollo 15 green glasses are thought to represent the composition of the primitive deep lunar mantle, its origin could be melting a hybridized source region (Longhi 1992), assimilation of LMO cumulates by another melt (Elkins-Tanton et al. 2003), or mixing of two different melts (Barr and Grove 2013). These hypotheses are still model-driven. The depth of its parental magmatic source may be constrained by multiple saturation experiments but also depends on the composition of lunar mantle cumulates, which are constrained by the bulk Moon composition, the depth of LMO, and the thermal condition deep inside the Moon.

2.1.2 Intermediate-Ti glasses

The yellow-brown ultramafic lunar glasses were found in samples returned from the Apollo 14, 15, and 17 landing sites. These glasses record a range of TiO_2 content from $\sim$ 3 wt% in the A15 samples to $\sim$ 7 wt% in the A17 samples (Brown and Grove 2015). Compared to the A15G, A15 yellow-brown glass has lower Ni abundances ($\sim$ 85 ppm) and lower Mg# ($\sim$ 49). Among these, A14 yellow glasses with $\sim$ 5 wt% TiO_2 is a typical intermediate-Ti glass.

Analysis of major- and trace-elements in A15 yellow-brown glasses suggested that the petrogenesis of these volcanic glasses can be unified into a set of partial melting processes of differentiated cumulates in the lunar mantle. A hybridization model explains their possible source regions does not require secondary assimilation of crustal material but requires a small amount of trapped late-stage intercumulus liquid besides melt from the early and later stage mantle cumulates derived from the evolution of the primordial LMO. And the intermediate-Ti mare magmas generates from deep ($\sim$ 400 km or more) regions in the lunar mantle (Hughes et al.1988). Later, Brown and Grove (2015) did some multiple saturation experiments to examine the original depth of A14 yellow glass. Their experimental results show that this yellow glass is in equilibrium with olivine and low-Ca pyroxene at a pressure between 2.4 and 3.0 GPa (or 512–646 km in depth) (Brown and Grove 2015). Meanwhile, the exact pressure/depth depends on the oxygen fugacity (f_{O_2}) during petrogenesis, and the multiple saturation point (MSP) moves to a greater depth at lower f_{O_2}. It is similar to the view of Hughes et al. (1988) above, they also suggested that mixing of remelted source cumulates and KREEP source, combined with small amounts of olivine fractionation, can reproduce yellow ultramafic lunar glasses. Lunar mantle overturn is the most likely process that reconciles the observed major- and trace-element compositional characteristics. Lunar mantle overturn brought the late-stage cumulates into greater depth inside the lunar mantle if the LMO was relatively shallow ($\sim$ 500 km). For the deeper LMO scenario (1000 km), the experimental determined MSP may represent the pressure of mixing of different melts. As mentioned above, the MSP experimental results are model-driven. Future experimental work on remelting, mixing LMO cumulates will help to further constrain the formation mechanism of lunar volcanic glasses.

In addition, some experiments were also conducted at pressures exceeding the maximum pressure of the lunar interior to gain further insight into the density and compressibility of the A14Y glass. The crossover of the density of A14Y and its equilibrium mineral assemblage at a pressure between 2.3 and 3.2 GPa indicate that the yellow

glass can rise through the mantle by buoyancy forces alone (Vander Kaaden et al. 2015). Although the original depth of the yellow-brown ultramafic lunar glasses determined from multiple saturation experiments is dependent on the LMO differentiation model, the observation that some ultramafic melts from similar depths but formed at different temperatures (Fig. 4) indicates the lunar interior is heterogeneous and the Moon went through a complex thermal history (Brown and Grove 2015).

2.1.3 High-Ti glasses

High-Ti volcanic glasses contain orange, red, and black glasses ranging in TiO_2 content from 9.12 to 13.8 to 16.4 wt%, respectively (Delano, 1986). Models for the origin of lunar high-Ti ultramafic glasses were either assimilation of late-stage clinopyroxene-ilmenite cumulates at a shallow level (Delano 1986; Wagner and Grove 1997) or mixing of melt from sinking clinopyroxene–ilmenite cumulate at depth (Hess 1991; Hess and Parmentier 1995; Ringwood and Kesson 1977). However, experimental work on the melting product of clinopyroxene–ilmenite source material showed that assimilation processes cannot account for the formation of lunar high-Ti glasses (Van Orman and Grove 2000). And for the mixing model, requires more work on the density difference between the high-Ti melt and the underlying mafic cumulate at different pressure and temperature conditions.

High pressure and high-temperature experiments showed that f_{O_2}) can affect the multiple saturation condition of high-Ti glasses with olivine and orthopyroxene. If f_{O_2} changed from $\Delta IW + 1.3$ to $\Delta IW -2.1$, the estimated minimum depth of origin of high-Ti glasses (red and orange) can shift about 300 km. And also, at pressures > 3.1 GPa, clinopyroxene (sub-calcic augite) and garnet are stable near the liquidus. The different mineral phases may have a key influence on the composition of the glass melt (Krawczynski and Grove 2012). In particular, the liquidus density of black glass is about 3.13 g/cm^3, which is the densest known magma in the solar system (Vander Kaaden et al. 2015). Delano (1986) pointed out that those lunar magmas with higher TiO_2 contents than A14B may be absent from the lunar surface. This prediction was confirmed by experimental studies by Circone and Agee (1996), which showed that the compressibility of molten high-TiO_2 black glass was large enough to make them denser at depth below 400 km and predicted it could not buoyant from an olivine–pyroxene source rock (Circone and Agee 1996; Delano 1986). However, these previous studies on lunar picritic melt density have not assessed buoyancy in the source region at their respective depths of origin. More recently, Vander Kaaden et al. (2015) reestablished realistic criteria for determining the buoyancy of glass liquids concerning their source regions, considering source mineralogy and average depths of melting. Their results showed that high Ti-rich liquid is nearly incompressible at a higher pressure and black glass should be able to buoyant to the crust-mantle boundary, but other modes are required to extract A17O melt composition from the mantle (Vander Kaaden et al. 2015). In addition, the density of various highland regions has been shown to vary from 2.59 to 2.87 g/cm^3 (Wieczorek et al. 2013), lower than those of high Ti-rich melt. Therefore, other processes, for example, volatile component degassing probably aid the eruption of these high-Ti melts through the lunar crust to the surface.

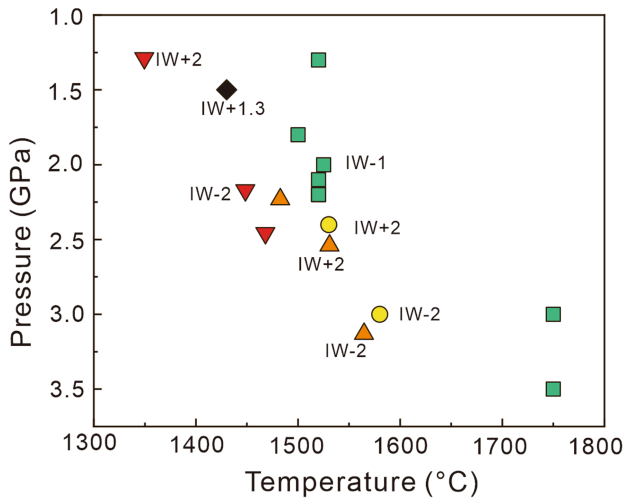

Fig. 4 Compilation of multiple saturation points of lunar ultramafic glasses. Oxygen fugacity and temperature both affect the depth of the source region of the lunar volcanic glasses. Different colors represent the colors of volcanic glasses. Data are from Barr and Grove (2013), Draper et al. (2006), Elkins-Tanton et al. (2003), Krawczynski and Grove (2012), and Wagner and Grove (1997)

2.2 Other constraints

The formation of lunar volcanic glasses is closely related to mare basalts and the age of volcanic glass highly overlaps with mare basalt (Table 2). Although remote sensing results and studies on lunar samples do not reflect a simple relationship between age and Ti content, the high-Ti glasses/basalts may be older than the low-Ti glasses/basalts (Brown and Grove 2015). However, it is not certain that all high-Ti basalts are old, for example, photogeologic data indicate that some high-Ti basalts may have erupted onto the lunar surface as recently as about 1.0 Ga ago (Schultz and Spudis 1983), these ages do provide insights into the evolving chemical nature and mechanisms of lunar volcanism and define the duration of volcanic activity on the Moon. Moreover, as stated above, oxygen fugacity has significant effects on the high-pressure phase equilibria of

Table 2 Age of partial lunar basalts and lunar volcanic glasses

Type	Age (Ga)
A15 GGs	3.35–3.41[a]
YBGs	3.62[a]
A 17 OGs	3.48[b]
Low-Ti (1–6 wt%), mare basalts	3.08–3.37[b]
A14 high-Al, low-Ti basalts	~ 3.95[c]
A11 high-Ti (> 6 wt%) basalts	3.55–3.86[b]
A17 high-Ti basalts	3.69–3.79[d]

A- Apollo, *GGs*- green glasses, *YBGs*- yellow-brown glasses, *OGs*- orange glasses

[a]Hughes et al. (1988); [b]Turner (1992); [c]Snape et al. (2019); [d]Norman et al. (2012)

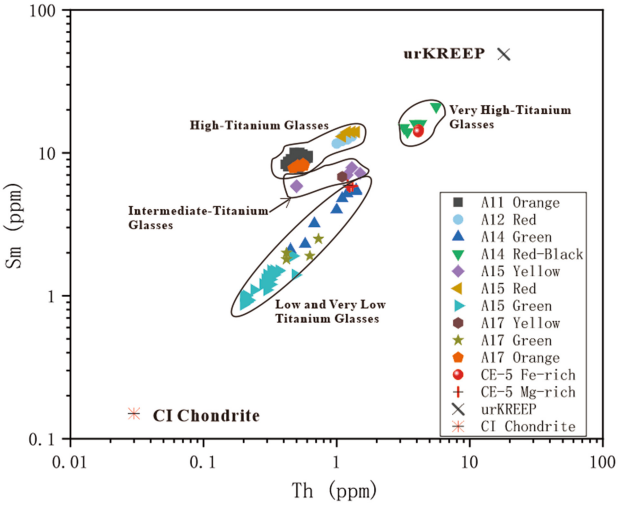

Fig. 5 Concentrations of Sm and Th in lunar pyroclastic glasses. Data are cited from Hagerty et al. (2006). Chang'e-5 (CE-5) glasses data are from this study

lunar glasses. Because titanium is very sensitive to oxygen fugacity, the depth range of source magma for high-Ti glasses is affected by oxygen fugacity more than that for low-Ti glasses. Some ultramafic melts from similar depths on the Moon were melted at very different temperatures under different oxygen fugacity conditions, indicating that these glasses have experienced very different thermal histories and the lunar interior is heterogeneous at a given depth (Fig. 4). Studying the formation mechanism, the origin depth, and the source mineral composition of lunar volcanic glasses will not only provide information about the migration of the material inside the Moon but also help to constrain the thermal history and the development of oxygen fugacity of the lunar interior through time.

In addition, it is noteworthy that the lunar samples returned from China's Chang'e-5 mission show that young mare basalts (~ 2.0 Ga) may originate from a KREEP-free and dry magmatic source (Hu et al. 2021; Li et al. 2021; Tian et al. 2021). The formation mechanism and the heat source for the generation of the young mare basalt remain unclear. Recently, we analyzed glasses in the Chang'e-5 sample (No. CE5C0800YJFM00101GP, hereafter "01GP"). The Sm and Th concentrations in the low-Ti (~2.21 wt%) and intermediate-Ti (~4.34 wt%) glasses in 01GP are different from that found in volcanic glasses of Apollo samples (Fig. 5). Considering the young age of Chang'e-5 basalt, it will be interesting to investigate how the Chang'e-5 samples can help to constrain the thermal evolution of the lunar interior.

3 Origin of Mg-suite

The lunar highlands' pristine igneous rocks were divided into two suites, the ferroan-anorthosite suite and the Mg-rich plutonic suite (James and Flohr 1983). However, not all pristine cumulates fit neatly into this classification. According to the petrographic, mineralogic, compositional, and isotopic data, Papike et al. (1998) subdivided the Mg-rich highlands rocks into the magnesian plutonic rocks (also known as Mg-suite or magnesian suite rocks), alkali rocks (also known as alkali-suite), and KREEP [lunar component high in potassium(K), Rare Earth Elements (REE), and phosphorus (P)] basalts (Papike et al. 1998). The Mg-suite is lithologically diverse with a range of rock types including ultramafics, troctolites, spinel troctolites, anorthositic troctolites, norites, and gabbronorites (Shearer et al. 2015). Based on analysis of Apollo lunar samples, the remote sensing data showed that the Mg-suite rocks are not uniformly distributed throughout the lunar surface but mainly concentrated in the Procellarum KREEP Terrane (PKT) platform (Jolliff et al. 2000; Longhi et al. 2010), which could explain the KREEP elemental characteristics of Mg-suite rocks. The Mg# of mafic minerals in Mg-suite can be as high as 95 ($Fo_{95–90}$) (Elardo et al. 2011; Shearer and Papike 2005), indicating a basaltic parental magma generated by high degree partial melting of the interior of the Moon, which was triggered by gravitational overturn or melt generated from the early crystallization products of LMO. The high An# of feldspars in Mg-suite indicates the residual magma with high Ca content or the melting of Ca-rich minerals (Fig. 6). On the other hand, Mg-suite rocks are dated older than 4.1 Ga, among the most ancient samples returned from the Moon (Carlson et al. 2014). Therefore, the primitive mineralogy combined with ancient ages indicates Mg-suite samples are representative products of post-lunar magma ocean overturn and can provide insight into the early lunar interior and magmatic migration process post-dating the differentiation of LMO.

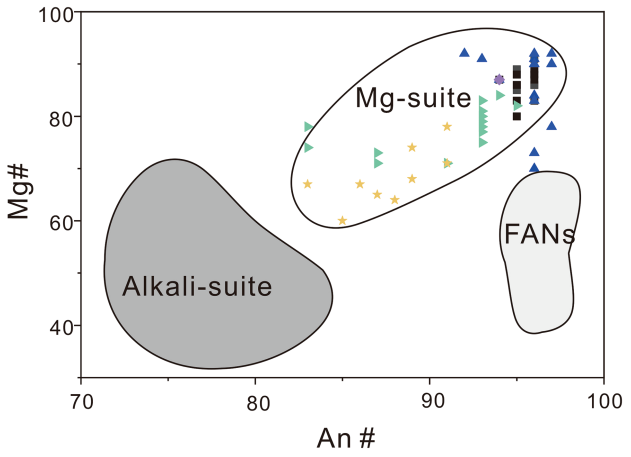

Fig. 6 Mg# in mafic silicates (olivine or opx) vs. An# in plagioclase for Mg-suite, Alkali-suite, and ferroan anorthosites (FANs). Modified from Shearer et al. (2015)

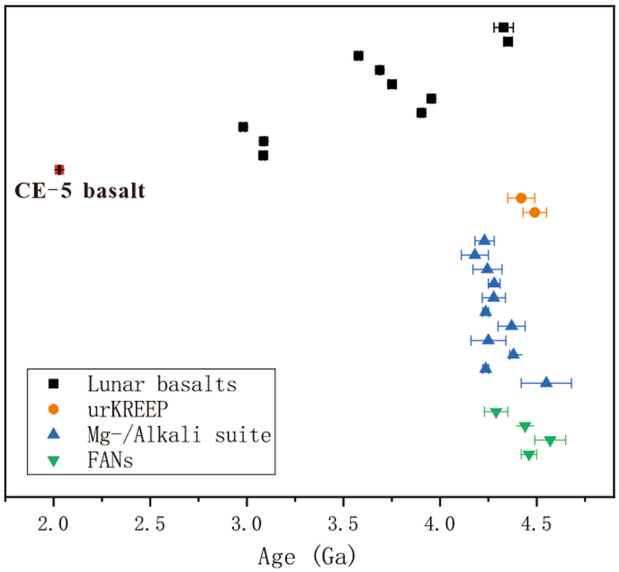

Fig. 7 Chronology of Mg-suite rocks compared to other highlands lithologies. Data are cited from Li et al. (2021) and Shearer et al. (2015)

3.1 Petrogenesis

There are significant differences in mineral and chemical composition between the Mg-suite and the ferrous anorthosites representing the lunar crust, indicating that these two rock composition units formed in different petrogenetic environments. It was suggested that the post-LMO magma intruded into primitive anorthositic crust and formed Mg-suite (Sun et al. 2017). Because of the radiogenic heat production and the ability of KREEP to lower the melting point of Mg-suite source rocks, we would expect considerably more crust-building magmatism on the nearside than on the far side of the Moon (Elardo et al. 2020). However, there are several problems with the formation mechanism of Mg-suite that are not well explained. First, olivine-dominated lithologies, which should be expected from the overturn model are lacking in the orbital and sample (lunar meteorites and returned lunar samples) database. Second, Mg-suite magmatism is supposed to be dated younger than the lunar ferroan crust, but the chronology of the Mg-suite overlaps with other highlands lithologies (e.g., FANs, alkali suite) (Fig. 7) (Shearer et al. 2015). Third, KREEP-poor lunar meteorites with Mg-suite-like mineralogy have been found in areas outside the PKT Terrane (Gross et al. 2020; Prissel et al. 2014), indicating that Mg-suite magmatism could be a global event that occurred without significant KREEP contribution.

Numerous petrogenetic models have been proposed to account for the formation of Mg-suite as reviewed by Shearer et al. (2015) (Fig. 8). (1) The "impact origin" model (Hess 1994) is abandoned because it cannot satisfy with mass balance issue and fails to crystallize high-Mg# mafic silicates. (2) The "magma ocean crystallization" model suggests that both Mg-suite and ferroan anorthosites are contemporaneous products of early crystallized

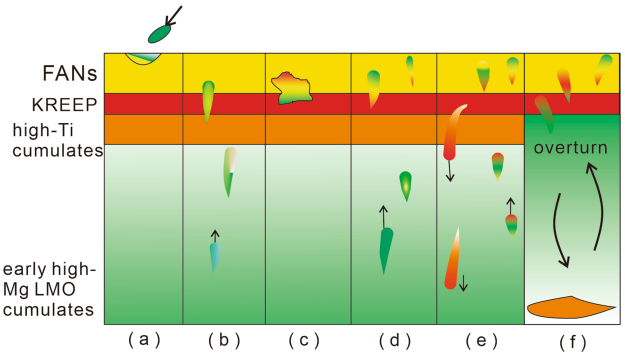

Fig. 8 Models for the formation of Mg-suite. **a** Impact formation through crystallization of melt sheets. **b** Co-crystallization of Mg-suite and FANs from the LMO. **c** Mobilization of urKREEP and emplacement into the lunar crust. **d** Assimilation of urKREEP ± FANs by Mg-rich magmas derived from early LMO cumulates. **e** Hybridization of early LMO cumulates by KREEP as a result of overturn of cumulate pile. **f** Hybridization and melting of early LMO cumulates at the base of the lunar crust. PKT- Procellarum KREEP Terrane; FHT- Feldspathic Highlands Terrane. Modified from Shearer et al. (2015)

accumulation and trapped melts of the magma ocean (McCallum 1983; Wood 1975), which can explain the overlapping ages for the Mg-suite rocks and the FANs. However, there is research indicating that the FANs cannot be generated from the same parental magma as the Mg-suite (Raedeke and McCallum 1980). (3) The "remelting and remobilization of late-stage magma ocean cumulates such as KREEP" model (Hess et al. 1978) (Fig. 8c) apparently cannot explain the primitive character of Mg-suite [e.g., high Mg# and high An#]. (4) The "assimilation

of KREEP, anorthositic crust, or both by melt from the lower portion of Al-rich cumulate" model (Warren and Wasson 1977) (Fig. 8d) can account for the fractionated incompatible element signature (high REE, fractionated Eu/Al), but Mg# of the hybrid melt is not consistent with that in Mg-suite (Hess 1994; Shearer and Papike 1999). Compared to the other models, the "Hybridization and melting of cumulate sources either in the deep (5) or shallow (6) lunar mantle" model (Elardo et al. 2011; Shearer 2006) (Fig. 8e and f) have obvious advantages to solve the Mg#, trace elements, and dynamical evolution problems. The hybridization occurred by melting cumulates in the deep mantle or at the base of the lunar crust via lunar mantle overturn. However, the cumulate overturn mechanisms are not identified for the transport of the less-dense urKREEP and high-Al crustal lithologies ($\rho < 2900$ kg/m^3) into the deep lower mantle (Shearer and Papike 1999; Shearer et al. 1991).

Experimental studies on the hybridized source region of Mg-suite demonstrated that the different initial Al_2O_3 content in the mantle-derived melt can cause the compositional difference in spinel in Mg-Suite (Prissel et al. 2016). Thus, different lunar Mg-suite rocks may form through different mechanisms from different source regions, for example, lunar troctolites may crystalize from mantle melt, while the existence of pink spinel in Mg-suite rocks indicates assimilation of lunar anorthositic crust.

3.1.1 Troctolite

Troctolites are the most abundant and thoroughly studied Mg-suite rock types that traditionally include norites along with rarer dunite, and a few gabbronorite clasts found in breccias may also be related (Shearer et al. 2015). The troctolite samples in Apollo collation and lunar meteorites are the most magnesium-rich with an average Mg# of 80–89, and a "small" amount of pink spinel troctolites ($\sim$ 2%) have Mg# up to 96. In general, troctolites are interpreted to be successive emplacements of mafic cumulate or melt into the crust soon after crystallization of LMO, therefore they are perhaps representative of the earliest stages of lunar magmatism (> 4.1 Ga) (Prissel and Gross 2020; Shearer et al. 2015). Prissel and Gross (2020) proposed an alternative formation mechanism for Mg-suite by modeling the petrogenesis of troctolite. Their modeling results show that the source magma of Mg-suite could be formed through a direct decompression melting of the mantle cumulate caused by mantle overturn, and does not need the addition of KREEP materials. Crystallization of the Mg-suite primary melt results in a range of mineralogy with the predominant constituents of the Mg-suite (common lunar troctolites and norites). And also, the Mg-suite primary melts may assimilate KREEP or interact with the anorthositic crust to produce pink spinel anorthosites and/or pink spinel troctolites (Fig. 9). In addition, this new model explains the formation of Mg-suite magma in the absence of an olivine-dominated upper mantle (Prissel and Gross, 2020). This hypothesis directly ties the Mg-suite crystallization ages to the onset and duration of lunar mantle overturn. The contemporaneous relationship between Mg-suite magmatism and melting of LMO solidification products caused by mantle overturn suggests that the mantle overturn started immediately after or during the end period of LMO solidification. This deduction is consistent with geophysical modeling results (Li et al. 2019; Morison et al. 2019; Zhao et al. 2019). However, this hypothesis redefined the Mg-suite differentiation trend with KREEP-free mantle-derived melts by assuming that these melts were extracted from their source region deep inside the lunar mantle. Based on their calculation, the Mg-suite primary melts are low degree partial melting of primitive olivine-rich lower mantle ($\sim$1.9% fractional melt at $\sim$2.1 GPa). The advection of partial melts to the base of the lithosphere should be efficient to avoid reaction with wall rock. What is the driving force for this small amount of melt to separate from their parental rock and rise quickly? It cannot be heated from the bottom of the LMO, because this will increase the temperature and may cause a large degree of partial melting. In addition, the melting simulation results show that garnet is exhausted when the melting degree is less than 2%, which is not consistent with our experimental results as mentioned previously. More experimental work needs to be done to test the modeling results.

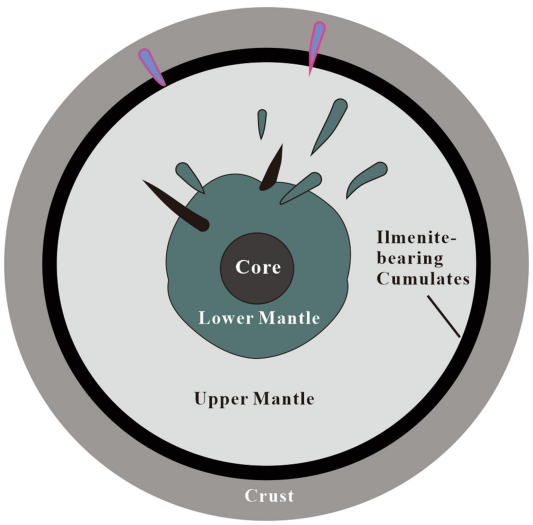

Fig. 9 Illustrations of the Mg-suite petrogenetic and mantle overturn hypothesis. Pink and Blue: Mg-suite. Refer to Prissel and Gross (2020) for more details

The model by Prissel and Gross (2020) also provides support and feasibility for the view that Mg-suite is one of the global crystallization products, as well as KREEP, is not a required component of Mg-suite petrogenesis. Our theoretical calculation model also supports this point of view. We choose different melting products of the lunar deep mantle cumulate at different depths as the source magma. Equilibrium crystallization and fractional crystallization products of these melts are calculated by the rhyolite-MELTS_v1.0.x program. Our modeling results show that fractional crystallization of the melt formed by batch melting or low degree partial melting of mantle cumulate can produce Mg-suite rocks and Anorthites (Fig. 10). KREEP is not involved in the process either (Ju et al. 2021).

Recently, we notice that the average Th content of the Chang'e-5 basalt is different from that found in lunar volcanic glasses, mare basalts, and FANs, but is similar to the Th content of the Mg-suite (Fig. 11). Therefore, it remains to be investigated whether the Chang'e-5 samples have new implications for the petrogenesis of Mg-suite.

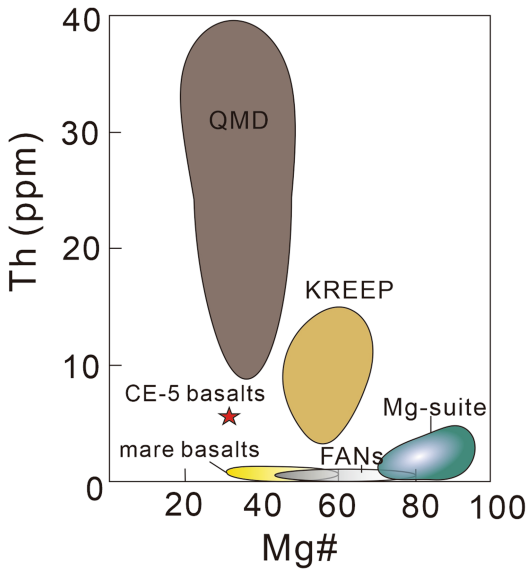

Fig. 11 Mg# vs. Th in a series of whole rock geochemical parameters. QMD: quartz-monzodiorites. Data are cited from Shearer et al. (2015) and Tian et al. (2021)

3.1.2 Pink Spinel (Mg-rich alumina spinel)

The Moon Mineralogy Mapper (M^3) onboard Chandrayaan-1 has identified a suite of highly unusual rock types exposed in small areas within the farside Moscoviense Basin and the nearside Theophilus crater (Dhingra et al. 2011; Pieters et al. 2011). The lithology appears to be dominated by anorthitic feldspar and is rich in "pink" spinel with mafic-free anorthosite, termed "pink spinel anorthosite" (PSA) (Dhingra et al. 2011). 38 Mg-spinel bearing craters were identified in 166 investigated lunar craters (Sun et al. 2017), indicating that Mg-rich spinel may be ubiquitous in the lunar crust.

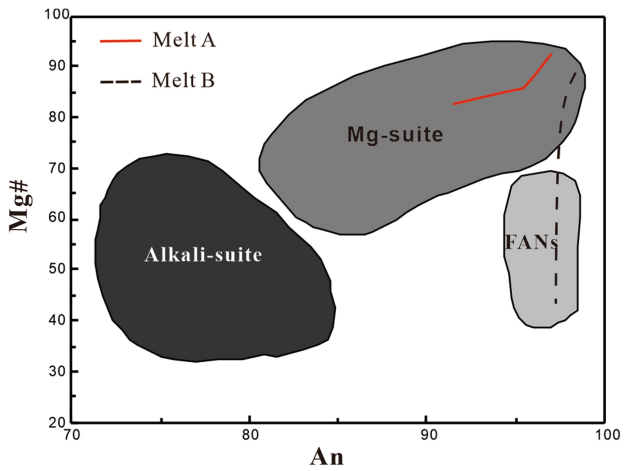

Fig. 10 Comparison of Mg# of olivine and An# of plagioclase in the crystallization products of melts from decompression melting. The melt A represents the partial melting, and the melt B represents the batch melting. Data is from Ju et al. (2021)

Gross and Treiman (2011) described a fragment containing ~30% (Mg, Fe)-spinel in lunar meteorite ALHA 81005, similar to the composition of PSA. The petrographic and chemical features of Al-rich spinel in ALHA 81005 are consistent with the regional setting of the Moscoviense spinel deposit, suggesting that they could have formed as a picritic magma body that assimilated crustal anorthosite on its margins (Gross and Treiman, 2011). The spectral signature of PSA is consistent with spinel having Mg# > 90 (Mg/[Mg + Fe] × 100) and Cr# < 5 (Cr/[Cr + Al] × 100). Experimental results show that the formation mechanism of PSA is best explained by the interaction between Mg-suite parental melts and anorthositic crust. Low-Ti or high-Ti glass compositions can also form Fe-rich spinel when reacting with anorthosite, but assimilation of the lunar crust by mare basalts and picritic lunar glasses composition cannot produce Fe and Cr depleted spinel (Prissel et al. 2014). Considering the extensive distribution, compositional relationship, and Mg-suite-related petrogenesis, PSA was suggested to be a new member of the Mg-suite rocks (Prissel et al. 2014). PSA has been observed to distribute on both the lunar nearside and farside, supporting the argument that KREEP is not necessary for the formation of Mg-suite.

Overall, after mineralogical and chemical analysis on more lunar samples, the types of Mg-suite have got expanded. The distribution of Mg-suite is no longer limited

to specific areas, such as the PKT region, but is more likely to be global. Mg-suite formed from mixed partial melting products of different parts of the Moon's interior. Assimilation of the lunar anorthitic crust by melt formed deep inside the Moon with the addition of KREEP only accounts for some specific types of the Mg-suite. Therefore, further studies on more Mg-suite samples are needed to reevaluate the thermal evolution history of the Moon interior and to modify the LMO evolution model.

4 Conclusions

Based on the evolution of the existing LMO models, basaltic magma is generated through partial melt of lunar mantle cumulate triggered by post-magma ocean overturn. However, the melting processes are quite complicated and not as straightforward as the model suggests. The composition of the basaltic magma is controlled by the material composition of the lunar mantle overturn of the ultramafic cumulates in the early stage of LMO and the depth of partial melting in the later stage. Those factors are directly related to the chemical composition and depth of LMO, and the LMO differentiation model.

The deep LMO model supports the stability of the high-pressure phase, such as garnet, inside the Moon. More experimental data are needed to quantify whether the Al-rich high-pressure phase has an important influence on the constitution and properties of the lunar mantle and whether its presence is helpful to explain the formation of HREE-depleted lunar glasses, and Ni, Co-depletion in Mg-suite samples. In addition, more work on the youngest mare basalts returned by Chang'e-5 is expected to help address fundamental questions on lunar chronology, basalt petrogenesis, thermal evolution, and the nature of PKT.

Acknowledgements This work was funded by the Strategic Priority Research Program of the Chinese Academy of Sciences (XDB 41000000), the National Natural Science Foundation of China (41773052, 41973058, 41603067, and 42003054), Key Research Program of Frontier Sciences, CAS (ZDBS-SSW-JSC007-10), and Technical Support Talent Program of Chinese Academy of Sciences, 2021.

Declarations

Conflict of interest On behalf of all authors, the corresponding author states that there is no conflict of interest.

References

Barr JA, Grove TL (2013) Experimental petrology of the Apollo 15 group A green glasses: melting primordial lunar mantle and magma ocean cumulate assimilation. Geochim Cosmochim Acta 106:216–230. https://doi.org/10.1016/j.gca.2012.12.035

Borg LE, Connelly JN, Cassata WS, Gaffney AM, Bizzarro M (2017) Chronologic implications for slow cooling of troctolite 76535 and temporal relationships between the Mg-suite and the ferroan anorthosite suite. Geochim Cosmochim Acta 201:377–391. https://doi.org/10.1016/j.gca.2016.11.021

Brown SM, Grove TL (2015) Origin of the Apollo 14, 15, and 17 yellow ultramafic glasses by mixing of deep cumulate remelts. Geochim Cosmochim Acta 171:201–215. https://doi.org/10.1016/j.gca.2015.09.001

Carlson RW, Borg LE, Gaffney AM, Boyet M (2014) Rb-Sr, Sm-Nd and Lu-Hf isotope systematics of the lunar Mg-suite: the age of the lunar crust and its relation to the time of Moon formation. Philos Trans Roy Soc Mathe PhysEng Sci 372(2024). https://doi.org/10.1098/rsta.2013.0246

Circone S, Agee CB (1996) Compressibility of molten high-Ti mare glass: evidence for crystal-liquid density inversions in the lunar mantle. Geochim Cosmochim Acta 60(14):2709–2720. https://doi.org/10.1016/0016-7037(96)00117-2

Delano JW (1979) Apollo 15 green glass: Chemistry and possible origin. In: 10th Lunar and Planetary Science Conference, pp 275–300

Delano JW (1986) Pristine Lunar glasses—criteria, data, and implications. J Geophys Res-Solid Earth Planet 91(B4):D201–D213. https://doi.org/10.1029/JB091iB04p0D201

Dhingra D, Pieters CM, Boardman JW, Head JW, Isaacson PJ, Taylor LA (2011) Compositional diversity at Theophilus Crater: understanding the geological context of Mg-spinel bearing central peaks. Geophys Res Lett, 38. https://doi.org/10.1029/2011gl047314

Drake MJ (1976) Evolution of major mineral compositions and trace-element abundances during fractional crystallization of a model lunar composition. Geochim Cosmochim Acta 40(4):401–411. https://doi.org/10.1016/0016-7037(76)90005-3

Draper DS, duFrane SA, Shearer CK, Dwarzski RE, Agee CB (2006) High-pressure phase equilibria and element partitioning experiments on Apollo 15 green C picritic glass: implications for the role of garnet in the deep lunar interior. Geochim Cosmochim Acta 70(9):2400–2416. https://doi.org/10.1016/j.gca.2006.01.027

Draper DS, Xirouchakis D, Agee CB (2003) Trace element partitioning between garnet and chondritic melt from 5 to 9 GPa: implications for the onset of the majorite transition in the martian mantle. Phys Earth Planet Inter 139(1–2):149–169. https://doi.org/10.1016/s0031-9201(03)00150-x

Du W, Han B, Clark SM, Wang Y, Liu X (2017) Raman spectroscopic study of synthetic pyrope–grossular garnets: structural implications. Phys Chem Miner 45(2):197–209. https://doi.org/10.1007/s00269-017-0908-z

Edmunson J, Borg LE, Nyquist LE, Asmerom Y (2009) A combined Sm-Nd, Rb-Sr, and U-Pb isotopic study of Mg-suite norite 78238: further evidence for early differentiation. Geochim Cosmochim Acta 73(2):514–527. https://doi.org/10.1016/j.gca.2008.10.021

Elardo SM, Draper DS, Shearer CK (2011) Lunar Magma Ocean crystallization revisited: bulk composition, early cumulate mineralogy, and the source regions of the highlands Mg-suite. Geochim Cosmochim Acta 75(11):3024–3045. https://doi.org/10.1016/j.gca.2011.02.033

Elardo SM, Laneuville M, McCubbin FM, Shearer CK (2020) Early crust building enhanced on the Moon's nearside by mantle melting-point depression. Nat Geosci 13(5):339–343. https://doi.org/10.1038/s41561-020-0559-4

Elkins-Tanton LT, Burgess S, Yin Q-Z (2011) The lunar magma ocean: reconciling the solidification process with lunar petrology and geochronology. Earth Planet Sci Lett 304(3–4):326–336. https://doi.org/10.1016/j.epsl.2011.02.004

Elkins-Tanton LT, Chatterjee N, Grove TL (2003) Experimental and petrological constraints on lunar differentiation from the Apollo 15 green picritic glasses. Meteorit Planet Sci 38(4):515–527. https://doi.org/10.1111/j.1945-5100.2003.tb00024.x

Fogel RA, Rutherford MJ (1995) Magmatic volatiles in primitive lunar glasses.1. Ftir and Epma analyses of Apollo 15 green and yellow glasses and revision of the volatile-assisted fire-fountain theory. Geochim Cosmochim Acta 59(1):201–215. https://doi.org/10.1016/0016-7037(94)00377-X

Gaffney AM, Borg LE (2014) A young solidification age for the lunar magma ocean. Geochim Cosmochim Acta 140:227–240. https://doi.org/10.1016/j.gca.2014.05.028

Gross J, Hilton A, Prissel TC, Setera JB, Korotev RL, Calzada-Diaz A (2020) Geochemistry and Petrogenesis of Northwest Africa 10401: a new type of the Mg-Suite Rocks. J Geophys Res-Planets 125(5). https://doi.org/10.1029/2019JE006225.

Gross J, Treiman AH (2011) Unique spinel-rich lithology in lunar meteorite ALHA 81005: Origin and possible connection to M-3 observations of the farside highlands.J Geophys Res-Planets 116. https://doi.org/10.1029/2011je003858

Head JW, Wilson L (1979) Alphonsus-type dark-halo craters: Morphology, morphometry and eruption conditions. Paper presented at the Proceedings of Lunar Planet Science Conference, 10

Hagerty JJ, Shearer CK, Vaniman DT, Burger PV (2006) Identifying the effects of petrologic processes in a closed basaltic system using trace-element concentrations in olivines and glasses: implications for comparative planetology. Amer Mineral 91(10):1499–1508. https://doi.org/10.2138/am.2006.2091

Hess PC (1991) Diapirism and the origin of high TiO_2 mare glasses. Geophys Res Lett 18(11):2069–2072. https://doi.org/10.1029/91gl02539

Hess PC (1994) Petrogenesis of lunar troctolites. J Geophys Res Planets 99(E9):19083–19093. https://doi.org/10.1029/94je01868

Hess PC, Parmentier EM (1995) A model for the thermal and chemical evolution of the moons interior—implications for the onset of Mare volcanism. Earth Planet Sci Lett 134(3–4):501–514. https://doi.org/10.1016/0012-821x(95)00138-3

Hess PC, Rutherford MJ, Campbell HW (1978) Ilmenite crystallization in non-mare basalt: Genesis of KREEP and high-Ti mare basalts. In: Proceedings 9th Lunar Science Conference, pp 705–724

Hiesinger H, Head JW (2006) New views of lunar geoscience: an introduction and overview. New Views Moon 60:1–81. https://doi.org/10.2138/rmg.2006.60.1

Hu S, He H, Ji J, Lin Y, Hui H, Anand M, Tartese R, Yan Y, Hao J, Li R, Gu L, Guo Q, He H, Ouyang Z (2021) A dry lunar mantle reservoir for young mare basalts of Chang'E-5. Nature. https://doi.org/10.1038/s41586-021-04107-9

Hughes SS, Delano JW, Schmitt RA (1988) Apollo-15 yellow-brown volcanic glass—chemistry and petrogenetic relations to green volcanic glass and olivine-normative Mare basalts. Geochim Cosmochim Acta 52(10):2379–2391. https://doi.org/10.1016/0016-7037(88)90295-5

James OB, Flohr MK (1983) Subdivision of the Mg-suite noritic rocks into Mg-gabbronorites and Mg-norites. J Phys Res 88(S02). https://doi.org/10.1029/JB088iS02p0A603

Jolliff BL, Gillis JJ, Haskin LA, Korotev RL, Wieczorek MA (2000) Major lunar crustal terranes: Surface expressions and crust-mantle origins. J Geophys Res Planets 105(E2):4197–4216. https://doi.org/10.1029/1999je001103

Ju DY, Du W, Li R, Pang RL (2021) Constraints on the source of the Lunar Mg-suite by thermodynamic simulation. Bull Mineral Petrol Geochem 40(5):1154–1165. https://doi.org/10.19658/j.issn.1007-2802.2021.40.078

Khan A, Maclennan J, Taylor SR, Connolly JAD (2006) Are the Earth and the Moon compositionally alike? Inferences on lunar composition and implications for lunar origin and evolution from geophysical modeling. J Geophys Res Planets 111(E12). https://doi.org/10.1029/2005je002608

Krawczynski MJ, Grove TL (2012) Experimental investigation of the influence of oxygen fugacity on the source depths for high titanium lunar ultramafic magmas. Geochim Cosmochim Acta 79:1–19. https://doi.org/10.1016/j.gca.2011.10.043

Li HY, Zhang N, Liang Y, Wu BC, Dygert NJ, Huang JS, Parmentier EM (2019) Lunar Cumulate Mantle Overturn: a model constrained by Ilmenite rheology. J Geophys Res Planets 124(5):1357–1378. https://doi.org/10.1029/2018je005905

Li QL, Zhou Q, Liu Y, Xiao Z, Lin Y, Li JH, Ma HX, Tang GQ, Guo S, Tang X, Yuan JY, Li J, Wu FY, Ouyang Z, Li C, Li XH (2021) Two billion-year-old volcanism on the Moon from Chang'E-5 basalts. Nature. https://doi.org/10.1038/s41586-021-04100-2

Lin Y, Tronche EJ, Steenstra ES, van Westrenen W (2017) Experimental constraints on the solidification of a nominally dry lunar magma ocean. Earth Planet Sci Lett 471:104–116. https://doi.org/10.1016/j.epsl.2017.04.045

Lognonne P (2005) Planetary seismology. Annu Rev Earth Planet Sci 33:571–604. https://doi.org/10.1146/annurev.earth.33.092203.122604

Longhi J (1992) Origin of picritic green glass magma by polybaric fractional fusion. Proc Lunar Planet Sci 22:343–353

Longhi J (2006) Petrogenesis of picritic mare magmas: constraints on the extent of early lunar differentiation. Geochim Cosmochim Acta 70(24):5919–5934. https://doi.org/10.1016/j.gca.2006.09.023

Longhi J, Durand SR, and Walker D (2010) The pattern of Ni and Co abundances in lunar olivines. Geochim Cosmochim Acta 74(2):784–798. https://doi.org/10.1016/j.gca.2009.10.001

Mallik A, Ejaz T, Shcheka S, Garapic G (2019) A petrologic study on the effect of mantle overturn: Implications for evolution of the lunar interior. Geochim Cosmochim Acta 250:238–250. https://doi.org/10.1016/j.gca.2019.02.014

McCallum IS (1983) Formation of Mg-rich pristine rocks by crustal metasomatism. Lunar Planet Sci XIV:473–474

Morison A, Labrosse S, Deguen R, Alboussière T (2019) Timescale of overturn in a magma ocean cumulate. Earth Planet Sci Lett 516:25–36. https://doi.org/10.1016/j.epsl.2019.03.037

Nakamura Y (2005) Farside deep moonquakes and deep interior of the Moon. J Phys Res 110(E1). https://doi.org/10.1029/2004je002332

Nakamura Y, Lammlein D, Latham G, Ewing M, Dorman J, Press F, Toksoz N (1973) New seismic data on state of deep lunar interior. Science 181(4094):49–51. https://doi.org/10.1126/science.181.4094.49

Neal CR (2001) Interior of the moon: the presence of garnet in the primitive deep lunar mantle. J Geophys Res Planet 106(E11):27865–27885. https://doi.org/10.1029/2000je001386

Nyquist LE, Shih CY (1992) The isotopic record of Lunar volcanism. Geochim Cosmochim Acta 56(6):2213–2234. https://doi.org/10.1016/0016-7037(92)90185-l

Papike JJ, Ryder G, Shearer CK (1998) Lunar samples. In: Planetary Materials, vol. 36 of Reviews in Mineralogy. Mineralogical Society of America, Washington, pp. E1–E234.

Pieters CM, Besse S, Boardman J, Buratti B, Cheek L, Clark RN, Combe JP, Dhingra D, Goswami JN, Green RO, Head JW, Isaacson P, Klima R, Kramer G, Lundeen S, Malaret E, McCord T, Mustard J, Nettles J, Petro N, Runyon C, Staid M, Sunshine J, Taylor LA, Thaisen K, Tompkins S, Whitten J (2011) Mg-spinel lithology: a new rock type on the lunar farside. J Phys Res 116. https://doi.org/10.1029/2010je003727

Prissel TC, Gross J (2020) On the petrogenesis of lunar troctolites: New insights into cumulate mantle overturn & mantle exposures in impact basins. Earth Planet Sci Lett, vol 551.

Prissel TC, Parman SW, Head JW (2016) Formation of the lunar highlands Mg-suite as told by spinel. Am Mineral 101(7):1624–1635. https://doi.org/10.2138/am-2016-5581

Prissel TC, Parman SW, Jackson CRM, Rutherford MJ, Hess PC, Head JW, Cheek L, Dhingra D, Pieters CM (2014) Pink moon: the petrogenesis of pink spinel anorthosites and implications concerning Mg-suite magmatism. Earth Planet Sci Lett 403:144–156. https://doi.org/10.1016/j.epsl.2014.06.027

Raedeke LD, McCallum IS (1980) A comparison of the fractionation trends in the lunar crust and the Stillwater complex. In: Proceeding of the conference on the Lunar highlands crust, pp 133–153

Rapp JF, Draper DS (2018) Fractional crystallization of the lunar magma ocean: updating the dominant paradigm. Meteorit Planet Sci 53(7):1432–1455. https://doi.org/10.1111/maps.13086

Ringwood AE (1975) Some aspects of minor element chemistry of Lunar Mare Basalts. Moon 12(2):127–157. https://doi.org/10.1007/Bf00577874

Ringwood AE, Kesson SE (1977) Basaltic magmatism and bulk composition of Moon. 2. Siderophile and volatile elements in moon, earth and chondrites—implications for Lunar origin. Moon 16(4):425–464. https://doi.org/10.1007/Bf00577902

Sato M (1979) The driving mechanism of lunar pyroclastic eruptions inferred from the oxygen fugacity behavior of Apollo 17 orange glass. In: Paper presented at the proceedings of the lunar and planetary science conference, p 10

Schultz PH, Spudis PD (1983) Beginning and end of lunar mare volcanism. Nature 302(5905):233–236. https://doi.org/10.1038/302233a0

Shearer CK, Papike JJ, Galbreath KC, Shimizu N (1991) Exploring the Lunar Mantle with Secondary Ion Mass-Spectrometry—a comparison of Lunar Picritic Glass-Beads from the Apollo-14 and Apollo-17 Sites. Earth Planet Sci Lett 102(2):134–147. https://doi.org/10.1016/0012-821×(91)90003-Z

Shearer CK, Papike JJ (1999) Magmatic evolution of the Moon. Amer Mineral 84(10):1469–1494. Retrieved from <Go to ISI>://WOS:000083078900001

Shearer CK (2006) Thermal and magmatic evolution of the moon. Rev Mineral Geochem 60(1):365–518. https://doi.org/10.2138/rmg.2006.60.4

Shearer CK, Elardo SM, Petro NE, Borg LE, McCubbin FM (2015) Origin of the lunar highlands Mg-suite: An integrated petrology, geochemistry, chronology, and remote sensing perspective. Amer Mineral 100(1):294–325. https://doi.org/10.2138/am-2015-4817

Smith JV, Anderson AT, Newton RC, Olsen EJ, Wyllie PJ (1970) Petrologic history of the Moon inferred from petrography, mineralogy, and petrogenesis of Apollo 11 rocks. In: Proceedings of Apollo 11 Lunar Science Conference, pp 897–925

Solomon SC, Head JW (1980) Lunar Mascon basins—lava filling, tectonics, and evolution of the Lithosphere. Rev Geophys 18(1):107–141. https://doi.org/10.1029/RG018i001p00107

Sun Y, Li L, Zhang YZ (2017) Detection of Mg-spinel bearing central peaks using M-3 images: implications for the petrogenesis of Mg-spinel. Earth Planet Sci Lett 465:48–58. https://doi.org/10.1016/j.epsl.2017.01.019

Taylor SR (1975) Lunar science; a PostApollo view. Pergamon, New York, p 372

Tian HC, Wang H, Chen Y, Yang W, Zhou Q, Zhang C, Lin HL, Huang C, Wu ST, Jia LH, Xu L, Zhang D, Li XG, Chang R, Yang YH, Xie LW, Zhang DP, Zhang GL, Yang SH, Wu FY (2021) Non-KREEP origin for Chang'E-5 basalts in the Procellarum KREEP Terrane. Nature. https://doi.org/10.1038/s41586-021-04119-5

Turner G (1992) Lunar sourcebook - a users guide to the moon - Heiken, Gh, Vaniman, Dt, French, Bm. Nature 358(6384):293–293. https://doi.org/10.1038/358293a0

Van Orman JA, Grove TL (2000) Origin of lunar high-titanium ultramafic glasses: constraints from phase relations and dissolution kinetics of clinopyroxene-ilmenite cumulates. Meteorit Planet Sci 35(4):783–794. https://doi.org/10.1111/j.1945-5100.2000.tb01462.x

Vander Kaaden KE, Agee CB, McCubbin FM (2015) Density and compressibility of the molten lunar picritic glasses: implications for the roles of Ti and Fe in the structures of silicate melts. Geochim Cosmochim Acta 149:1–20. https://doi.org/10.1016/j.gca.2014.10.029

Wagner TP, Grove TL (1997) Experimental constraints on the origin of lunar high-Ti ultramafic glasses. Geochimica et Cosmochimica Acta 61(6):1315–1327. https://doi.org/10.1016/S0016-7037(96)00387-0

Walker D, Hays JF (1977) Plagioclase flotation and lunar crust formation. Geology 5(7):425–428. https://doi.org/10.1130/0091-7613(1977)5<765:IOHBOA>2.0.CO;2

Warren PH (1985) The Magma ocean concept and Lunar evolution. Annu Rev Earth Planet Sci 13:201–240. https://doi.org/10.1146/annurev.ea.13.050185.001221

Warren PH, Wasson JT (1977) Pristine nonmare rocks and the nature of the lunar crust. In: Proceedings 8th Lunar science conference, pp 2215–2235

Weber RC, Lin PY, Garnero EJ, Williams Q, Lognonne P (2011) Seismic detection of the Lunar core. Science 331(6015):309–312. https://doi.org/10.1126/science.1199375

Wieczorek MA, Neumann GA, Nimmo F, Kiefer WS, Taylor GJ, Melosh HJ, Phillips RJ, Solomon SC, Andrews-Hanna JC, Asmar SW, Konopliv AS, Lemoine FG, Smith DE, Watkins MM, Williams JG, Zuber MT (2013) The crust of the moon as seen by GRAIL. Science 339(6120):671–675. https://doi.org/10.1126/science.1231530

Wood JA (1972) Thermal history and early magmatism in Moon. Icarus 16(2):229. https://doi.org/10.1016/0019-1035(72)90070-X

Wood JA (1975) Lunar petrogenesis in a well-stirred magma ocean. In: Proceedings 6th Lunar science conference, pp 1087–1102

Wood JA, Dickey JS, Marvin UB, Powell BN (1970) Lunar anorthosites and a geophysical model of the Moon. In: Proeedings of Apollo 11 Lunar Science conference, pp 965–988.

Yao L, Liang Y (2012) An experimental study of the solidus of a hybrid lunar cumulate mantle: Implications for the temperature at the core-mantle boundary of the Moon. In: Paper presented at the lunar and Planetary Institute Science Conference.

Zhao Y, de Vries J, van den Berg AP, Jacobs MHG, van Westrenen W (2019) The participation of ilmenite-bearing cumulates in lunar mantle overturn. Earth Planet Sci Lett 511:1–11. https://doi.org/10.1016/j.epsl.2019.01.022